Hierarchy of Symbolic Computer-Generated Real-Time Vehicle Dynamics Models

MICHAEL W. SAYERS AND PAUL S. FANCHER

Symbolic multibody code generation technology enables a new approach for developing vehicle models for driving simulators. Rather than assembling terms in the equations of motion, a modeler can concentrate on modeling issues such as degrees of freedom (df), joint constraints, and kinematical assumptions. An automated code generator makes it practical to test many modeling assumptions to determine their influence on computation time and simulation fidelity, leading to a model that offers the most fidelity while running in real time on available hardware. The new methodology is illustrated by (a) describing seven vehicle handling models, with various levels of complexity, ranging from 4 to 10 df; (b) comparing the computational requirements for their use; and (c) presenting example comparisons of predicted motions. All of the models can be simulated in real time on a fast personal computer. The simplest (4-df) model runs more than 40 times faster than the more complex 10-df one, yet it predicts overall vehicle motions that agree closely. Among the 10-df models, the fastest runs 2.3 times quicker than the slowest. The methodology illustrated can be used to extend the models to include additional mechanical characteristics of interest.

Driving simulators are not in widespread use, even though they are acknowledged as highly useful research tools for human factors and psychology studies. Recent technical developments make the development of driving simulators much simpler than has ever been possible. Computer hardware has improved so much that even desktop computers with graphical capabilities have the speed and software needed to generate simple scenes in response to driver motions. A system consisting of a mock-up dashboard or car interior, computer, and visual display can now be assembled for a fraction of the cost required a few years ago. Complementing the hardware improvements are new software technologies that can be used to develop suitable vehicle dynamics models.

The purpose of this paper is to use these new software technologies to show quantitatively the effects of modeling assumptions used in familiar vehicle dynamics models with different levels of complexity (*1–6*). Comparisons are made on the bases of computational speed and accuracy.

All of the mathematical models described in this paper were developed using AUTOSIM, a software package that automatically derived equations of motion for mechanical systems composed of multiple rigid bodies. The AUTOSIM software has been described previously (*7,8*). The models presented are not new and have also been described before. By combining an automated equation generator with a set of vehicle models, it is possible to compare the models quantitatively. In this paper, the focus is on the kinematics of the various models. The goal is to demonstrate a general method for using new technology involving the dynamics of multibody systems and the automatic generation of symbolic computer codes for simulating vehicle dynamics.

This paper illustrates a new way of thinking about models—not as a set of equations, but as physical connections with degrees of freedom (df), constraints, and their kinematical interpretations.

NEW MULTIBODY SIMULATION TECHNOLOGY (AUTOSIM)

AUTOSIM is a symbolic code generator that reads text input describing the model and produces source code as output in one of the supported computer languages (FORTRAN, C, MATLAB, ACSL, and ADSIM). Parameters are represented by symbols, so that the same equations can be applied many times without changing the equations themselves. Persons wishing to try the ideas presented in this paper can license AUTOSIM commercially in North America from Mitchell and Gauthier Associates in Concord, Massachusetts, and, for other countries, from University of Michigan Software, in Ann Arbor.

The method of developing models with a symbolic multibody program provides several novel advantages:

- Equations are written in terms of parameters chosen by the modeler instead of a fixed set of multibody parameters.
- The multibody program is used only to develop the model. Once the equations are written, the model can be exercised directly to answer questions of interest.
- The time needed to develop a self-contained simulation code is very short (typically, a few hours—a time that might not appear possible to persons with experience in developing models by other methods).
- AUTOSIM usually generates equations that are more efficient than those developed by any other method, including hand derivations made by experts. It uses an advanced form of Kane's equations (*9*) and then applies extensive algebraic and programming optimization methods to achieve high efficiency. [See work by Sayers (*10*) for comparisons of AUTOSIM formulations with those obtained by other methods, including hand-derivation, for several models.]

University of Michigan Transportation Research Institute, 2901 Baxter Road, Ann Arbor, Mich. 48109.

- The generated source code is completely accessible for inspection and modification.
- Hand-written subroutines and auxiliary variables can be easily included in models.
- An interactive multibody program lets the modeler rapidly develop and inspect equations to debug the model and evaluate alternative modeling assumptions.

The mathematical basis of for this technology has been described previously (*7,8*), and example uses of the technology in support of a comprehensive vehicle system dynamics model for a driving simulator have been presented (*11,12*).

Communicating with AUTOSIM entails describing the system to be simulated on the computer. In general terms, the software is structured around a geometric description of the system, involving matters such as the connections between bodies and the locations of the joint connections, the centers of mass, and the action of the forces. Developing a model with the new technology clearly involves different tactics than developing a model with pencil and paper. Mathematical matters that otherwise might be given a great deal of attention have been reduced to computer algorithms, freeing the modeler from some past burdens.

The rest of this paper uses the type of thinking that goes into the development of a vehicle model when using a symbolic multibody program. Alternative models are developed for a vehicle system, using a fixed set of basic vehicle parameters. Modeling decisions are described explicitly, and the effects are shown quantitatively in terms of the complexity of the resulting equations and the accuracy of the model predictions.

MODEL DESCRIPTIONS

Vehicle Description

For purposes of comparison, a hierarchy of vehicle models is defined, from complex to simple. The models are formulated to calculate the vehicle response to steer inputs when running on a smooth and level surface at a constant speed. Table 1 gives the complete set of parameters used in the models. The vehicle being considered is a front-wheel-drive compact with a solid rear axle and independent front suspension with unequal upper and lower control arms. To help isolate the significance of assumptions that reduce the kinematical complexity, areas of behavior that are not of primary interest are left out of the models or greatly simplified. The models will be compared under conditions of constant forward speed, therefore longitudinal tire forces are not included. Details of how control inputs from the driver cause the wheels to steer are not considered: the control inputs in the models are simply the steer of the front wheels. Aerodynamic effects are ignored. Suspension and tire matters are treated in the following discussions.

Suspension Kinematics

TABLE 1 Vehicle Parameters

Symbol	Value	Description
C_{A1}	880N/deg	front cornering stiffness, one tire
C_{A2}	880N/deg	rear cornering stiffness, one tire
C_{S1}	600 N-s/m	front shock absorber damping (1 wheel)
C_{S2}	600 N-s/m	rear shock absorber damping (1 wheel)
F_{ZA1}	880 kg	front axle load (2 wheels)
F_{ZA2}	550 kg	rear axle load (2 wheels)
H	0.51 m	height of sprung mass c.g. above the ground
H_{RC1}	0.0 m	height of front suspension roll center
H_{RC2}	0.25 m	height of rear suspension roll center
I_{XX}	330 kg-m2	moment of inertia of S
I_{YY}	1300kg-m2	moment of inertia of S
I_{ZZ}	2000 kg-m2	moment of inertia of S
K_G	5 deg/m	change in wheel inclination with vertical position
K_{S1}	26000 N/m	front suspension vertical stiffness (1 wheel)
K_{S2}	26000 N/m	rear suspension vertical stiffness (1 wheel)
K_{SWAY1}	600 m-N/deg	auxiliary anti-roll stiffness for front
K_{SWAY2}	50 m-N/deg	auxiliary anti-roll stiffness for rear
K_{T1}	175000 N/m	front tire vertical stiffness (1 wheel)
K_{T2}	175000 N/m	rear tire vertical stiffness (1 wheel)
L	2.5 m	wheelbase
M_{A1}	120 kg	front unsprung mass (2 wheels)
M_{A2}	90 kg	rear unsprung mass (2 wheels)
R_1	0.3 m	front tire rolling radius
R_2	0.3 m	rear tire rolling radius
S_2	0.6 m	rear spring spacing
T_1	1.4 m	front track
T_2	1.4 m	rear track

Figure 1 shows a simplified front view of the front suspensions, with the dimensions T_1, R_1, and H_{RC1}. The figure also shows a linkage analysis of the independent suspension on the right-hand wheel that locates an instant center. (For small vertical movements of the wheel, the motions are as if the wheel is attached to a rigid body that rotates about the instant center.) By considering a simple rotation, it is easy to visualize small roll-plane motions of the wheel and determine such properties as how the camber and track (distance between tire centers) change with suspension deflection. The instant center is also a point at which the net moment applied to the car body by the suspension is 0. Thus, any force acting on the wheel whose line of action passes through the instant center does not apply a moment to the car body. The figure shows a line connecting the instant center with the center of the contact patch between the tire and the road. The moment applied to the car body as a result of a tire force vector is determined by the orientation of the vector relative to this line. Because of symmetry, a similar analysis for the other front wheel leads to the identification of a single point that is at the intersection of the lines connecting the tire contact patch centers with the corresponding instant centers. The intersection point is called the roll center. The instant centers and roll center are "paper points" that do not correspond to any physical connections. Their locations depend on the actual position of the unsprung masses. Thus, the instant centers, and the roll center, can change position as the suspensions move.

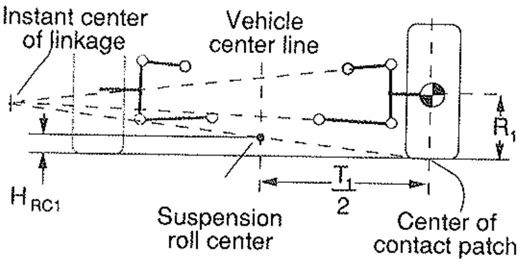

FIGURE 1 Front suspension.

The mass center for the suspension subsystem (wheel, spindle, and suspension links) is shown at the center of the wheel. In general, the mass center is not at this point, although it is close. The approximation is made to reduce the number of parameters.

Figure 2 shows the corresponding view for the rear axle. For simplicity, a leaf-spring suspension is shown. However, the same dimensions (T_2, S_2, and H_{RC2}) could be used for any suspension with a solid axle. Here, the leaf springs react lateral forces such that the net moment applied to the sprung mass is 0 along a line connecting the attachments of the springs to the body. [The role-center analyses illustrated in Figures 1 and 2 are brief and simple. More detailed analyses can be found elsewhere for a variety of suspension types (*13*).]

Fully detailed suspension descriptions are usually inappropriate for low-cost real-time driving simulators. Simplified representations, as will be presented, have been used in models that have been validated through comparison with experimental handling tests. In all of the models that follow, suspension kinematics are simplified. The degree of simplification depends on the model.

Suspension Force Elements

Linkages shown in Figures 1 and 2 control the motions permitted between the sprung and unsprung masses. In addition, springs and dampers connect the bodies. In both the front and rear, each side has a spring with a force deflection relation

$$F_{\text{spring}} = f_{\text{static}} + f_s(\delta) \qquad (1)$$

where δ is the spring deflection and f_{static} is the static load carried by the spring. Each suspension may have auxiliary forces applied as functions of relative roll, due to antisway bars and linkage compliances. This effect results in a force acting between the two wheels on the same suspension, and has the general form

$$F_{\text{roll}} = f_r(\delta_L - \delta_R) \qquad (2)$$

where, in this case, δ_L and δ_R are movements of the left and right wheels relative to the body. The suspensions also include shock absorbers that produce force as a function of shock absorber displacement rate:

$$F_{\text{damper}} = f_d(\dot{\delta}) \qquad (3)$$

The displacements and rates appearing in these equations (δ, δ_L, δ_R, and $\dot{\delta}$) are derived from the kinematics of the moving rigid bodies by AUTOSIM. The force laws, expressed by the functions f_s, f_d, and f_r, can be arbitrarily complex nonlinear relationships. In this paper, simple linear relations are used. The spring forces are computed using linear coefficient K_{S1} and K_{S2} for the front and rear springs, the damping forces are computed using linear coefficients C_{S1} and C_{S2} for front and rear dampers, and the auxiliary roll force is computed with a linear relation

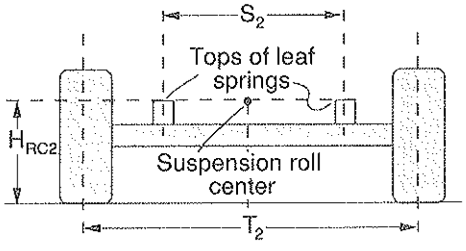

FIGURE 2 Rear axle.

$$F_{\text{roll}} = 57.3\,\frac{K_{\text{SWAY}}}{S}\,(\delta_L - \delta_R) \qquad (4)$$

where K_{SWAY} and S are as defined in Table 1.

The baseline set of parameters shows a spring spacing for the front suspension equal to the track. This means that the spring and damper rates are effective at the wheel plane. None of the models represents the relative displacement of a coil spring in a double A-arm suspension, and therefore the forces predicted by the different models do not agree unless the spring spacing is set equal to the track. To apply spring or damper data to any of these models, a separate analysis is needed to convert the true force and deflection to the effective force and deflection at the wheel plane. This is an application of a multibody program that has been described elsewhere (*11*).

Tire Forces and Moments

The most important actions affecting a vehicle being steered at constant speed are the vertical tire forces and lateral shear forces. Experiments have established that the vertical and lateral tire forces are essentially functions of just a few variables. The vertical force (normal to the ground surface) has the form

$$F_Z = f_{\text{static}} + f_z(\delta, \gamma) \qquad (5)$$

where δ is tire deflection (from the static condition) and γ is tire inclination angle. The relation that will be used for all models in this paper is

$$F_Z = -g\,\frac{F_{ZA}}{2} - K_T\delta_T \qquad (6)$$

where F_{ZA} and K_T are parameters defined in Table 1 for front and rear wheels and δ_T is the change in the distance from the center of the wheel to the center of the contact patch between the tire and ground. An expression for δ_T is derived by AUTOSIM for each wheel in a model, on the basis of multibody kinematics. (The negative sign is to satisfy the SAE coordinate system, in which the vertical Z-axis points down.)

When running at constant speed with no longitudinal forces from braking or acceleration, lateral tire force is a function of vertical load and a few kinematical variables:

$$F_Y = f_y(F_Z, \alpha, \gamma, V, \mu) \qquad (7)$$

where

α = slip angle (angle between direction a rolling tire is pointing and direction of velocity vector of a point in wheel plane where it meets ground),

γ = inclination angle of wheel,
V = forward speed of rolling tire, and
μ = friction coefficient.

The vertical load is determined by Equation 6, α and γ are determined by multibody kinematics, and μ is a parameter. [The slip angle, α, is sometimes given a time delay to account for the need for the tire to roll a certain distance, called the relaxation length, to build up a lateral force (*14*).] For all of the models that will be presented, a very simple relation is used to determine lateral tire force:

$$F_Y = -57.3\ C_A\alpha \tag{8}$$

This model omits significant influences, particularly those of load (F_Z) and inclination angle (γ). The omissions are made to simplify the comparisons between the different models. The F_Z values predicted by the different models are compared to show the form of inputs available to a sophisticated tire model if one were to be used.

Models that are developed and compared in the following will not include aerodynamic effects or longitudinal tire forces that occur when braking. Tire moments will not be considered either.

Summary of Models

There are many ways to model a vehicle to include the elements described and predict vehicle motions in response to control inputs. Four multibody models were developed to describe a vehicle with the characteristics just described. Furthermore, equations were formulated for the first model using four variations. Thus, seven formulations were obtained.

Models 1a Through 1d: 10-df Models with Translational Joints

The first three models (1a, 1b, and 1c) are similar to the Highway-Vehicle Object System Model (HVOSM), developed two decades ago for mainframe and hybrid computers (*5*). They have 10 pertinent df: 6 for the sprung mass (the car body), 2 for the rear axle, and 1 each for the two front independent suspensions. The independent suspensions are modeled by assuming that the wheel unsprung masses move relative to the car body as if they were connected with purely translational joints, as shown in Figure 3. Although the translational joint in the figure is shown at a slant to add generality, in the original HVOSM model and in Models 1a, 1b, and 1c, the direction of the translation is parallel to the vertical axis of the sprung mass. In the AUTOSIM program, this kinematical relationship is described by defining each front wheel/suspension body as being connected to the sprung mass and as having a single allowable translational motion, parallel to the Z-axis of the sprung-mass coordinate system. The simple translational motions, permitted each wheel, approximate the motion of the front suspension.

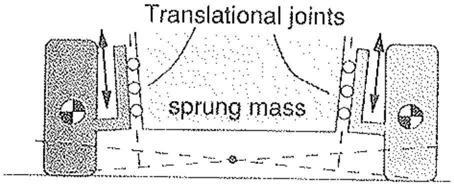

FIGURE 3 Multibody representation of front suspensions for Model 1.

When the lateral tire forces, applied in the road plane, are reacted completely by the translational joint, they do not apply a roll moment to the car body. However, the simple kinematical analysis shown in Figure 1 indicates that the double-arm suspension applies a net moment of 0 only at the roll center. The two cases are not equivalent unless the suspension roll center is at the ground plane, as is the case for the nominal parameter values given in Table 1. (The original HVOSM model was modified to include additional terms, called jacking forces, to generate the correct reaction forces and moments between the wheel and car bodies).

The multibody representation of the rear axle is shown in Figure 4. A massless intermediate body is connected to the sprung mass at the roll center. The unsprung mass, consisting of a rigid body with the axle, wheels, tires, and the like lumped together, is connected to the intermediate body with a purely translational joint.

The tire deflections and slip angles are defined by considering vectors defined in a coordinate system of a wheel spindle rigid body. Consider the geometry shown in Figure 5. The inertial coordinate system is defined by X-, Y-, and Z-axes whose directions are shown in the figure. The directions are defined mathematically by unit vectors $\mathbf{n}_x$, $\mathbf{n}_y$, and $\mathbf{n}_z$. Three unit vectors are also fixed in the moving reference frame of the spindle: $\mathbf{s}_x$, $\mathbf{s}_y$, and $\mathbf{s}_z$. Point S is at the center of the wheel, Point O is a point fixed in the ground plane, and Point C is defined such that it is in the local Z-direction ($\mathbf{s}_z$) of the spindle, relative to Point S, and it coincides with the ground plane. The position vector going from Point S to Point C is

$$\mathbf{r}^{SC} = r\mathbf{s}_z \tag{9}$$

The fact that Point C lies in the ground plane is expressed mathematically by the condition

$$\mathbf{r}^{OC} \circ \mathbf{n}_z = 0 \tag{10}$$

where $\mathbf{r}^{OC}$ is the position vector connecting Points O and C. Noting that

$$\mathbf{r}^{OC} = \mathbf{r}^{OS} + \mathbf{r}^{SC}$$

the local Z-coordinate of Point C (r in Equation 9) can be

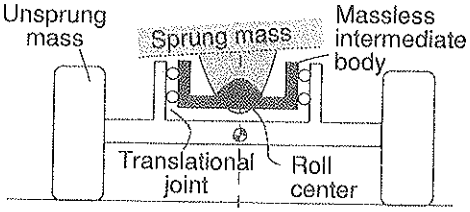

FIGURE 4 Multibody representation of rear axle for Model 1.

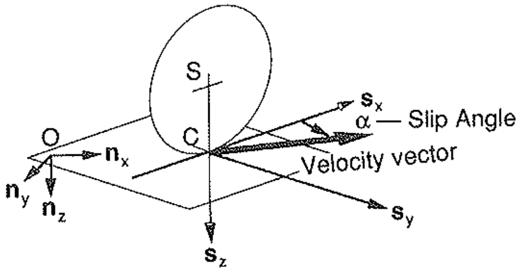

FIGURE 5 Geometry of slip angle.

defined as

$$r = -\frac{\mathbf{r}^{OS} \cdot \mathbf{n}_z}{\mathbf{s}_z \cdot \mathbf{n}_z} \tag{11}$$

The tire deflection δ_T, appearing in Equation 6, is simply

$$\delta_T = r - \bar{r} \tag{12}$$

where $\bar{r}$ is the value of r when the system is in its nominal configuration.

The rigorous geometric definition of slip angle, α, is the angle between the vector projection of $\mathbf{s}_x$ onto the road plane and the absolute velocity vector of Point C, $\mathbf{v}_C$:

$$\alpha = \text{angle}\{[\mathbf{s}_x - (\mathbf{s}_x \cdot \mathbf{n}_z)\mathbf{n}_z], \mathbf{v}^C\} \tag{13}$$

where angle(•) is a function that determines the angle between two vectors and $[\mathbf{s}_x - (\mathbf{s}_x \cdot \mathbf{n}_z)\mathbf{n}_z]$ is the projection of s_x onto the ground plane. Model 1a uses this definition of slip.

When this definition for the slip angle is used as an input, AUTOSIM derives a lengthy formula that fills several pages. A considerably more simple formulation is obtained by changing the definition slightly to consider the angle in the plane perpendicular to the vector $\mathbf{s}_z$:

$$\alpha' = \text{angle}\{[\mathbf{s}_x, \mathbf{v}^C - (\mathbf{v}^C \cdot \mathbf{s}_z)\mathbf{s}_z]\} \tag{14}$$

Although these two formulations for slip angle appear very similar, it will be seen that the second one improves the simulation performance by about 50 percent. The reason is that the formulation in Equation 13 includes the local velocity of C in the reference frame of the wheel spindle. The local velocity component, in the $\mathbf{s}_z$ direction, is eliminated in the second formulation. Models 1b, 1c, and 1d use Equation 14 to define slip.

When formulating equations for mechanical systems, modelers often use knowledge that some movements are "small" to simplify the equations. AUTOSIM also has this capability (*8*). Model 1c was produced by declaring to AUTOSIM that certain motions are small. (Except for forward speed and yaw angle, the translations and rotations for all df were declared as small in Model 1b, thereby producing Model 1c.)

Models 1a, 1b, and 1c involve all of the parameters in Table 1 except two: the front roll center height, H_{RC1}, and the change in wheel inclination with vertical position, K_G.

A fourth variation, Model 1d, was defined by describing inclined directions for the translational joints as shown in Figure 3. For Models 1a, 1b, and 1c, the direction of the translation was defined as being purely in the Z-direction of the sprung mass, $\mathbf{s}_z$. For Model 1d, the direction $\mathbf{d}_r$ was specified as

$$\mathbf{d}_r = \frac{T_1}{2}\mathbf{s}_z \pm H_{\text{RC1}}\mathbf{s}_y \tag{15}$$

When the parameter H_{RC1} is assigned a value of 0, the two formulations are equivalent. However, because the equations for Model 1d include terms for the condition that H_{RC1} is not 0, the full equations are more complex.

Model 2: 10-df Model with Rotational Front Suspension Joints

The second model is identical to the Model 1c, except in the treatment of the front suspensions. Figure 6 shows the multibody representation of the geometry of the front wheel spindles. The instant center of rotation, a "paper point" shown in Figure 1, is used as the physical point of attachment between the unsprung and sprung masses. The model shown in Figure 6 defines the transfer of roll moments between the unsprung and sprung masses that is correct when the suspension is at the nominal (design) position. The model also predicts the first-order change in wheel camber angle with suspension deflection.

This model requires two dimensional parameters to locate the instant center: a lateral coordinate and a vertical one. These two dimensions are not common ones for vehicle dynamics models. However, they can be defined in terms of two commonly used parameters: roll center height, H_{RC1}, and a coefficient for the linear change in inclination angle with respect to vertical movement, K_G (see Table 1). The lateral distance from the wheel plane to the instant center is given by

$$L_{\text{ICY}} = \frac{57.3}{K_G} \tag{16}$$

and the height of the instant center above the ground plane is

$$H_{\text{IC}} = 2H_{\text{RC1}}\frac{L_{\text{ICY}}}{T_1} \tag{17}$$

As was done for Model 1c, all motion variables except the forward speed and the yaw angle are declared as small. Slip angles were defined by Equation 14. This model involves every parameter given in Table 1.

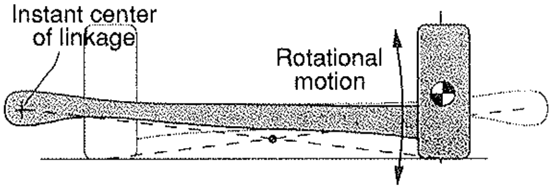

FIGURE 6 Multibody representation of front suspensions for Model 2.

Model 3: 6-df Model

This model has 6 df and is similar in pertinent respects to the VDANL model (*2,4*). Three df involve planar movement of a vehicle reference frame (X- and Y-translations and yaw rotation). The moving reference frame has front and rear roll centers, about which the front and rear unsprung masses roll. The geometry, shown in Figure 7, is as if the vehicle has two solid axles that rotate independently about a longitudinal axis passing through the respective roll centers. The sprung mass rolls relative to the reference frame as if it were connected by a hinge whose axis passes through both roll centers (see Figure 8). The body and two axles each add a roll df to the system, bringing the total to 6.

The equations derived for this model were made after specifying that the roll angles (and rates) and the lateral velocity are small. All of the parameters in Table 1 are used in this model, except K_G.

To describe the model in terms of the parameters of Table 1, all of the points needed to define the spring, damper, and tire forces are introduced. Because the AUTOSIM descriptions of forces from the tires, springs, and dampers depend on the relative movements of the reference points, the descriptions used for the 10-df models were repeated without modification to describe this model.

Model 4: 4-df Model

This model is similar to the 3-df model developed and validated by Segel in the 1950s (*6*) and embellished since then in many variations (*1*). Kinematically, the model is nearly identical to Model 3, except that the front and rear axles are not permitted to roll. Thus, all suspension motions are lumped into a single rotational df of the sprung mass about the roll axis. To maintain compatibility with the other models, torsional stiffness and damping coefficients are defined in terms of the parameters in Table 1. The torsional stiffness for each suspension $i(i = 1, 2)$, $K_{\text{susp}i}$, and each pair of tires, $K_{\text{tire}i}$ ($N - m$/rad), can be written

$$K_{\text{susp1}} = 57.3\ K_{\text{SWAY1}} + \frac{T_1^2\ K_{S1}}{2} \tag{18}$$

$$K_{\text{susp2}} = 57.3\ K_{\text{SWAY2}} + \frac{S_2^2\ K_{S2}}{2} \tag{19}$$

$$K_{\text{tire}i} = \frac{T_i^2\ K_{Ti}}{2} \qquad \text{for } i = 1, 2 \tag{20}$$

An overall torsional stiffness for each axle, with effects of both suspensions and tires being treated as springs in series, is then defined as

$$K_{\text{tors}i} = \frac{1}{\dfrac{1}{K_{\text{susp}i}} + \dfrac{1}{K_{\text{tire}i}}} \qquad \text{for } i = 1, 2 \tag{21}$$

A torsonal damping coefficient for each axle is defined as

$$C_{\text{tors1}} = \frac{T_1^2\ C_{S1} K_{\text{tors1}}}{2\ K_{\text{susp1}}} \tag{22}$$

$$C_{\text{tors2}} = \frac{S_2^2\ C_{S2} K_{\text{tors2}}}{2\ K_{\text{susp}i}} \tag{23}$$

where the ratio $K_{\text{tors}i}/K_{\text{susp}i}$ is used to scale the torsional damping to be representative of the level of shock absorber motion.

The total roll moment acting on the sprung mass, from both Axles 1 and 2, is

$$M_{\text{roll}} = -(K_{\text{tors1}} + K_{\text{tors2}})\phi - (C_{\text{tors1}} + C_{\text{tors2}})\dot{\phi} \tag{24}$$

Although the tire behavior assumed for all models in this paper does not include the effect of load on lateral shear force, the ability of the models to predict vertical tire load would of interest if a load-sensitive tire model were to be used. With the 4-df model, the vertical tire force can be written

$$F_Z = \frac{F_{ZA}}{2} \pm \frac{M_{\text{roll}}}{T} \tag{25}$$

MODEL PERFORMANCE

Each model was described as an AUTOSIM input. AUTOSIM then generated a ready-to-run FORTRAN simulation program for that model. The simulation programs take nearly identical inputs (the parameters shown in Table 1) and integrate ordinary differential equations to obtain motions of

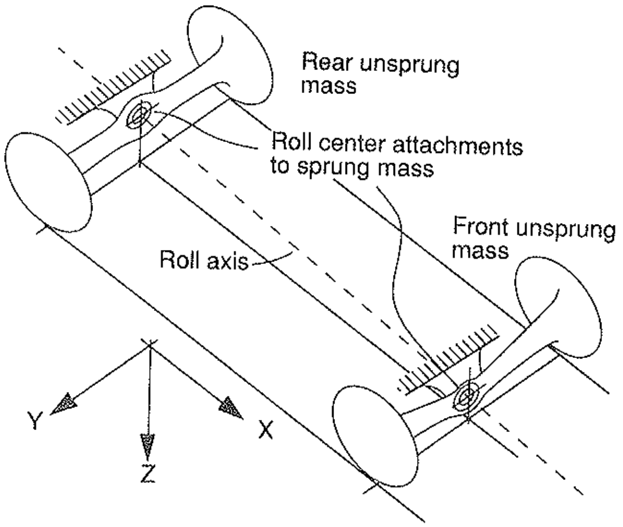

FIGURE 7 Joints used to build the 6-df model.

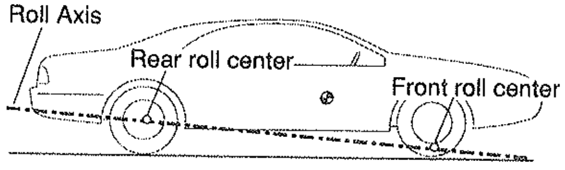

FIGURE 8 Vehicle roll axis.

the vehicle in response to a steer input of the front wheels. The number of equations corresponds to the number of state variables, which is twice the number of df for all of these models. (Each df is associated with one position variable and one speed variable.)

Computational Efficiency

When used in a driving simulator, the first and foremost requirement of the vehicle simulation is that it be capable of running in real time on the available hardware. Table 2 presents a summary of the computational aspects of the models. The main computational effort is spent computing the derivatives of the state variables. The three columns in the table for computation effort show the number of operations needed to compute the derivatives each time step. These computations are performed in a single subroutine that is repeatedly invoked in the loop by the numerical integration algorithm. Table 2 gives the number of multiply, divide, and exponent operations (*, /), the number of add and subtract operations (+, −), and the number of function and subroutine calls (funcs) such as sines, cosines, and absolute values. During their derivation, the equations are manipulated by AUTOSIM to avoid redundant computations and to precompute expressions involving constants. Auxiliary calculations that are not needed to compute derivatives each time step are not included in the table.

A second-order, fixed-step Runge-Kutta algorithm was selected as an integrator for all models. It causes the derivatives be calculated twice each time step, at the start and midpoint of the intervals shown in the table. The time steps shown in the table were selected by first finding the time step at which integration error could be discerned by visual inspection of plotted time histories and then cutting that time step in half. For example, Model 2 and all versions of Model 1 gave no noticeable error for a time step of 0.014, but all were unstable with a time step of 0.016. Therefore, the "safe" time step was set to 0.014/2 = 0.007 sec.

To give an approximate idea of the real running time, each model was timed on a Macintosh II fx. The simulated times were divided by the run times to yield a normalized speed in units of real time. (A factor of 1.3 means that the computer program runs 1.3 times faster than needed for real-time simulation with the time step shown. By increasing the time step, the program can be run up to 2.6 times faster than real time, where it borders on the limit of numerical integration stability.) The standard of what is real time clearly depends on the computer hardware. The results shown are intended not to link absolute simulation speeds with the models, but to show how the models compare relative to each other and to give at least an approximate idea of the types of absolute computational speed that would be expected from a "fast" personal computer made in 1990.

Table 2 shows that all 10-df models require a time step of 0.007 sec. Although only two of the first five models run faster than real time with the conservative time steps shown, all can be run in real-time within limits of stability. Model 3, with 6 df, runs more than three times faster than real time. Although it requires a time step almost as short as the 10-df models, it is described by equations of motion that are much simpler. Model 4, with 4 df, is 24 times faster than real time. The equations of motion are an order of magnitude simpler than the equations for the other models, and the dynamic system includes only low-frequency eigenvalues. Consequently, a much larger integration time step can be used to further reduce the computational requirements.

Numerical Results

All of the simulation programs were used to compute vehicle response to a simple ramp-to-step input for a right turn, shown in Figure 9. The steer angle is applied at the front wheels, eliminating any dynamic effects of the vehicle steering system. The forward speed is 30 m/sec (108 km/hr). The overall vehicle motions predicted by the different models agree closely. Plots of the responses from all five of the 10-df models were in-

TABLE 2 Comparison of Model Formulations

			Computation effort			time	run
Model	DOF[a]	Notes	*,/	+,−	funcs	step	speed*
1a	10	Similar to HVOSM, translational joints in Z direction for front suspensions, full non-linear kinematics, exact slip equations from eq. (13)	831	780	27	0.007	0.56
1b	10	Same as 1a except with slip defined in eq. (14)	540	514	21	0.007	0.85
1c	10	Same as 1b except with some "small" angles and speeds	335	386	5	0.007	1.3·
1d	10	Same as 1c except translational joints are angled to fit roll center	416	459	7	0.007	1.05
2	10	Same as 1c except with rotational joints for front suspensions	515	548	5	0.007	0.91
3	6	Similar to STI model	155	162	3	0.008	3.1
4	4	Similar to Segel model	34	22	5	0.020	24

* Note: run speeds are shown as multiples of real time on a Macintosh II fx running under Macintosh System 7.

[a] DOF = df.

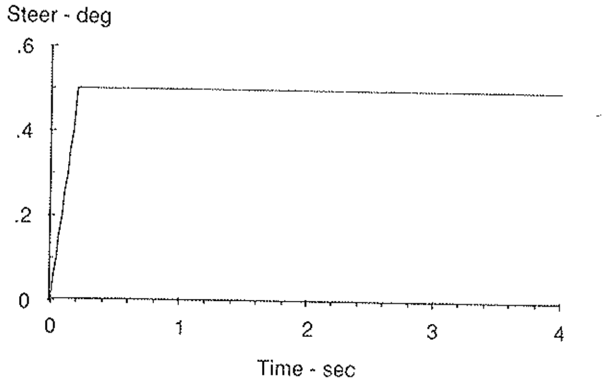

FIGURE 9 Steer input at front wheels.

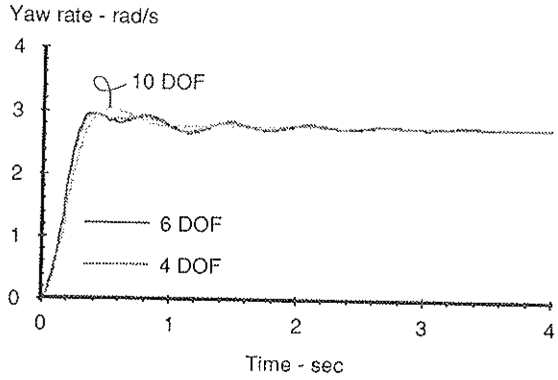

FIGURE 11 Predicted yaw rate responses.

distinguishable. Figure 10 shows that predictions of lateral acceleration were nearly identical for all models. Figure 11 shows that yaw rate predictions for the 4- and 6-df models do not completely match the prediction from the 10-df models. However, the predictions from the two simpler models agree with each other. The greatest difference in predicted vehicle motion was found for roll angle, shown in Figure 12. (However, even these differences are minor.) The main difference is that the 10-df models predict a slightly less oscillatory roll response.

The 4-df model is the simplest and fastest running. Because it does not directly account for roll of the axles, exact agreement in roll is not obtained. However, the results are not far off. Other than roll angle, the other predictions from the 4-df model are very close to those from the 10-df models.

The disagreement between the 10-df and simpler models was found to be mainly due to the different ways in which the models couple roll between the sprung and unsprung masses. The difference exists only when the roll centers at the front and rear differ, such that the vehicle roll axis is tilted. One factor associated with the tilt is that products of inertia are introduced in the simpler models that amplify the transient roll response. A second factor is that due to axle pushing in the 10-df models, shown in Figure 13. When the sprung mass rolls, the rear axle is constrained to move in the direction of the body roll, whereas the front axle moves in the opposite direction. The lateral movements of the axles modify the slip angles, instantly changing the lateral forces generated by the tires. The effect is to add damping to the 10-df model that is not present in the 4- and 6-df models.

The axle-pushing mechanism in the 10-df models may be exaggerated because of the simple tire model of Equations 8 and 13 or 14. In reality, lateral tire forces do not build instantly. A tire model with dynamic lag or lateral compliance might change the significance of the kinematic "pushing."

Recall that most of the 10-df models with translational joints for the front wheels have a front roll center in the ground plane (Models 1a, 1b, and 1c), whereas Models 1d and 2 locate a roll center whose height is defined as the parameter H_{RC1}. When H_{RC1} is set to 0, all of the 10-df models agree so closely that identical time history plots are obtained for any given response variable. However, differences exist for values of H_{RC1} other than 0. In this case, Models 1d and 2 compare closely with the simple models, and Models 1a, 1b, and 1c generate an incorrect roll response.

Although the simulation results in this paper are based on a tire equation that is not sensitive to load, all of the models can be easily extended to include load sensitivity in the lateral tire force calculations. Figure 14 compares the vertical force time histories for the right front tire. The 6-df and 10-df models agree closely, and the 4-df model produces estimates that may be sufficient to capture the rudimentary handling effects of tire load sensitivity.

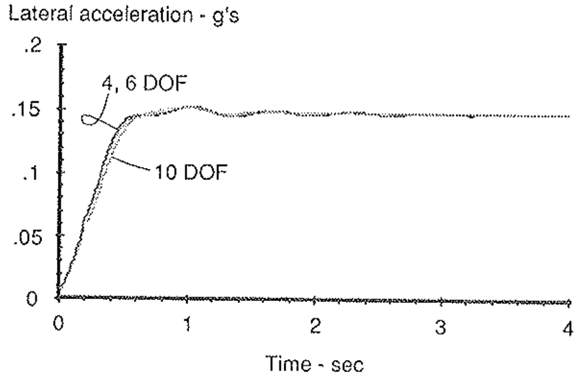

FIGURE 10 Predicted lateral acceleration responses.

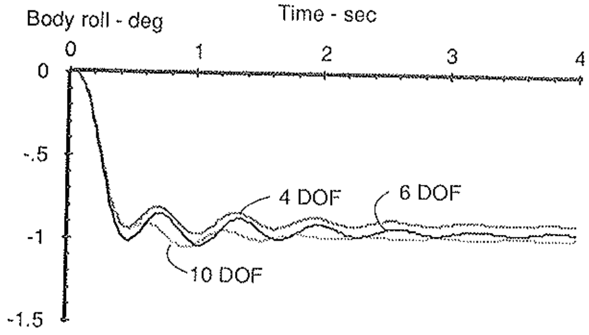

FIGURE 12 Predicted roll angle responses.

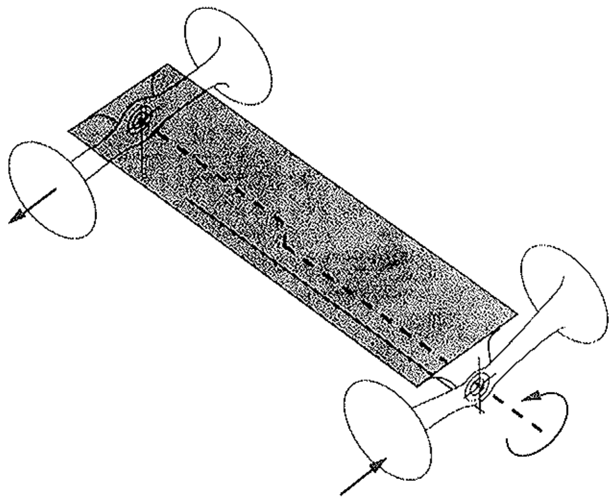

FIGURE 13 Front and rear suspension roll axes that are not collinear.

CONCLUSIONS

This paper shows how a symbolic multibody code generator is used to rapidly develop real-time vehicle dynamics models. Making comparisons between the models was easy, because all of the models were formulated using the same sets of vehicle parameters. The simplest simulation program runs more than 40 times faster than the most complex, yet the predictions of the overall system response were very close. The general approach of building simulation programs with a code generator has several advantages over the use of hand-coded programs:

- The development time is small. The first working 10-df model reported in this paper was developed and debugged in 2 days. The other 10-df models required less time. The initial versions of the 4- and 6-df models were done in several hours.
- The generated code runs fast. For a given model, the automated software for developing simulations usually formulates efficient equations and then generates code that is as fast or faster than that which can be written by experts (*10*).
- Models with different levels of complexity can be formulated and compared, to speed the debugging process and ensure that the modeling assumptions have the intended results.
- A model can be rapidly fine-tuned to run with maximum detail in real time on available hardware. Radical changes can be made in connection between bodies with little effort.

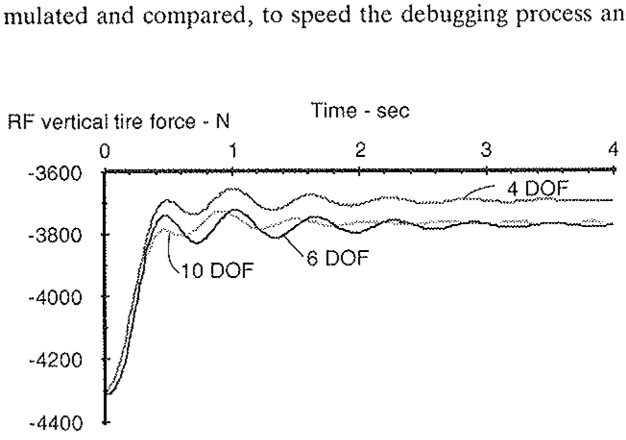

FIGURE 14 Vertical tire forces simulated by models.

The capability of a simulation program to run in real time depends on the computational efficiency in the equations of motion and the minimal integration time step required. The relatively close agreement seen between the simple 4-df model and the others argues that simple multibody models, with no high-frequency eigenvalues, offer a sound basis for building low-cost driving simulators. Complexities can be added such as roll steer, compliance steer, steering system dynamics, aerodynamic effects, nonlinear tire behavior, load-sensitive tires, dynamic tire lags, nonlinear springs and dampers, and so on. The model runs so fast that there is plenty of room for additional computations if they do not affect the required minimal time step.

ACKNOWLEDGEMENT

The authors wish to thank Ric Mousseau of Ford Motor Company for identifying the significance of the "axle push" behavior.

REFERENCES

1. R. W. Allen, T. J. Rosenthal, and H. T. Szostak. Steady State and Transient Analysis of Ground Vehicle Handling. Paper 870495. In *SAE Special Publication 699*, SAE, Warrendale, Pa., 1987, pp. 49–78.
2. R. W. Allen, T. J. Rosenthal, and H. T. Szostak. *Analytical Modeling of Driver Response in Crash Avoidance Maneuvering: Volume I: Technical Background.* DOT HS-807-270, NTIS 77225. U.S. Department of Transportation, 1988.
3. R. W. Allen, T. J. Rosenthal, D. H. Klyde, K. J. Owens, and H. T. Szostak. Validation of Ground Vehicle Computer Simulations Developed for Dynamics Stability Analysis. Paper 920054. In *SAE Special Publication 909*, SAE, Warrendale, Pa., 1992, pp. 59–78.
4. G. J. Heydinger. *Vehicle Dynamics Simulation and Metric Computation for Comparison with Accident Data.* DOT HS-807-828, NTIS 82367. U.S. Department of Transportation, 1991.
5. F. Jindra. *Mathematical Model of Four-Wheeled Vehicle for Hybrid Computer Vehicle Handling Program.* DOT HS-801-800, NTIS 33658. U.S. Department of Transportation, 1975.
6. L. Segel. Theoretical Prediction and Experimental Substantiation of the Response of the Automobile to Steering Control. *Proc., Institute of Mechanical Engineers Automobile Division*, 1957, pp. 310–330.
7. M. W. Sayers. Symbolic Vector/Dyadic Multibody Formalism for Tree-Topology Systems. *Journal of Guidance, Control, and Dynamics*, Vol. 14, No. 6, 1991, pp. 1240–1250.
8. M. W. Sayers. Symbolic Computer Language for Multibody Systems. *Journal of Guidance, Control, and Dynamics*, Vol. 14, No. 6, 1991, pp. 1153–1163.
9. T. R. Kane and D. A. Levinson. *Dynamics, Theory and Applications.* McGraw-Hill Series in Mechanical Engineering. McGraw-Hill Book Company, New York, 1985.
10. C. W. Mousseau, M. W. Sayers, and D. J. Fagan. Symbolic Quasi-Static and Dynamic Analyses of Complex Automobile Models. *Proc., 12th International Association for Vehicle System Dynamics Symposium on the Dynamics of Vehicles on Roads and on Tracks*, Lyon, France, Aug. 1991.

11. M. W. Sayers and C. W. Mousseau. Real-Time Vehicle Dynamic Simulation Obtained With a Symbolic Multibody Program. *Proc., 2nd Symposium on Transportation Systems at the Winter Annual Meeting* (J. Y. Wong, J. J. Moskwa, and S. A. Velinsky, eds.), American Society of Mechanical Engineers, Dallas, Tex., Nov. 1990.
12. T. D. Gillespie. *Fundamentals of Vehicle Dynamics*. SAE, Warrendale, Pa., 1992.
13. G. J. Heydinger, W. R. Garrott, and J. P. Chrstos. The Importance of Tire Lag on Simulated Transient Vehicle Response. Paper 910235. In *SAE Special Publication 861*, SAE, Warrendale, Pa., 1991, pp. 49–62.
14. M. W. Sayers. *Symbolic Computer Methods To Automatically Formulate Vehicle Simulation Codes*. Ph.D. dissertation. University of Michigan, Ann Arbor, Feb. 1990.

Publication of this paper sponsored by Committee on Simulation and Measurement of Vehicle and Operator Performance.